Ultrafast Electron Relaxation Dynamics in Coupled Metal Nanoparticles in Aggregates

Prashant K. Jain, Wei Qian, and Mostafa A. El-Sayed*

Laser Dynamics Laboratory, School of Chemistry and Biochemistry, Georgia Institute of Technology, Atlanta, Georgia 30332-0400

Received: September 29, 2005; In Final Form: November 3, 2005

We report the effect of aggregation in gold nanoparticles on their ultrafast electron−phonon relaxation dynamics measured by femtosecond transient absorption pump−probe spectroscopy. UV−visible extinction and transient absorption of the solution-stable aggregates of gold nanoparticles show a broad absorption in the 550−700-nm region in addition to the isolated gold nanoparticle plasmon resonance. This broad red-shifted absorption can be attributed to contributions from gold nanoparticle aggregates with different sizes and/or different fractal structures. The electron−phonon relaxation, reflected as a fast decay component of the transient bleach, is found to depend on the probe wavelength, suggesting that each wavelength interrogates one particular subset of the aggregates. As the probe wavelength is changed from 520 to 635 nm across the broad aggregate absorption, the rate of electron−phonon relaxation increases. The observed trend in the hot electron lifetimes can be explained on the basis of an increased overlap of the electron oscillation frequency with the phonon spectrum and enhanced interfacial electron scattering, with increasing extent of aggregation. The experimental results strongly suggest the presence of intercolloid electronic coupling within the nanoparticle aggregates, besides the well-known dipolar plasmon coupling.

I. Introduction

Nobel metal nanoparticles are fascinating materials with great nanotechnological potential because of their unique and strongly size-dependent electronic, chemical, and optical properties.[1,2] In the past few years there has been a strong interest in the self-assembly of nanoparticles into 1D chains,[3] dense 2D and 3D superlattices,[4] and Langmuir−Blodgett films.[5] The Alivisatos and Mirkin groups have developed protocols for assembling Au nanoparticles based on site-selective DNA hybridization.[6,7] Various experiments on such assembled systems have shown the emergence of novel physical properties due to the interaction between nanoparticles.[8,9] There is a great motivation to exploit the unique properties of these assembled materials for electronic and optical device applications. A great deal of effort has been devoted to the study of the optical properties of such nanoparticle assemblies. Nanoparticle assemblies with very short interparticle separations (comparable to the nanoparticle size) show a whole new absorption band in the 600−950-nm region in addition to the nanoparticle plasmon absorption because of strong internanoparticle interaction.[10−12] Interparticle interactions regulate various linear and nonlinear optical properties, for example, surface-enhanced Raman scattering (SERS),[9,13] two-photon absorption (TPA), and four-wave mixing (FWM), of nanoparticles embedded in matrices or assembled into thin films at a high volume fraction.[14]

It has been suggested that many applications of materials assembled from metal nanoparticles might be based upon their ultrafast response to optical excitation. They show promise as optical switches[15] and also as hot electron sources for photoelectrochemical processes, for example, solar energy conversion or organic waste reduction.[16] For applications such as these, it would be ideal to be able to tune their optical response and excitation lifetime. Tunability would be especially useful in the case of hot electron transfer to an electron acceptor where, to be effective, the electron cooling process should be slower than the time scale required for trapping and relaxation by the electron acceptor.[17] It is essential to have a detailed understanding of the electron dynamics in such nanoparticle assemblies before such applications can be realized.

Optical excitation of the conduction electrons in metal nanoparticles (without appreciable heating of the nanoparticle lattice) by means of ultrashort laser pulses has emerged as a powerful tool for probing the electron dynamics within these systems.[18,19] The energy of the photoexcited electrons is rapidly (within a few hundred femtoseconds) spread over the entire electron distribution via electron−electron scattering.[20] Comprehensive information about electron−electron scattering in conducting metals may be found in Kaveh et al.[21] and the references contained therein. The excited or "hot" Fermi electron distribution subsequently relaxes by exchanging energy with the nanoparticle lattice phonon modes (known as electron−phonon relaxation) on the time scale of few picoseconds. This is followed by phonon−phonon heat flow to the surrounding medium proceeding to equilibrium in several picoseconds, depending on the nanoparticle size and the thermal conductivity of the surrounding medium.[22−24]

The electron−phonon relaxation process in colloidal gold nanoparticles has been well studied by femtosecond pump−probe spectroscopic techniques in our lab[24−26] as well as other groups[27,28] and has been found to be on the time scale of ∼1 ps (at the lower limit of the excitation laser power), similar to that in bulk gold. The electron−phonon relaxation time was observed to be independent of the size or shape of the nanoparticles in these studies.[25−28] However, Del Fatti et al.,[29] Stella et al.,[30] Nisoli et al.,[31] and Perner et al.[32] observed size-dependent electron−phonon relaxation dynamics in silver, gallium, and tin nanoparticles.

* Corresponding author. E-mail: mostafa.el-sayed@chemistry.gatech.edu. Tel: 404-894-0294. Fax: 404-894-0292.

10.1021/jp055562p CCC: $33.50
Published on Web 12/10/2005

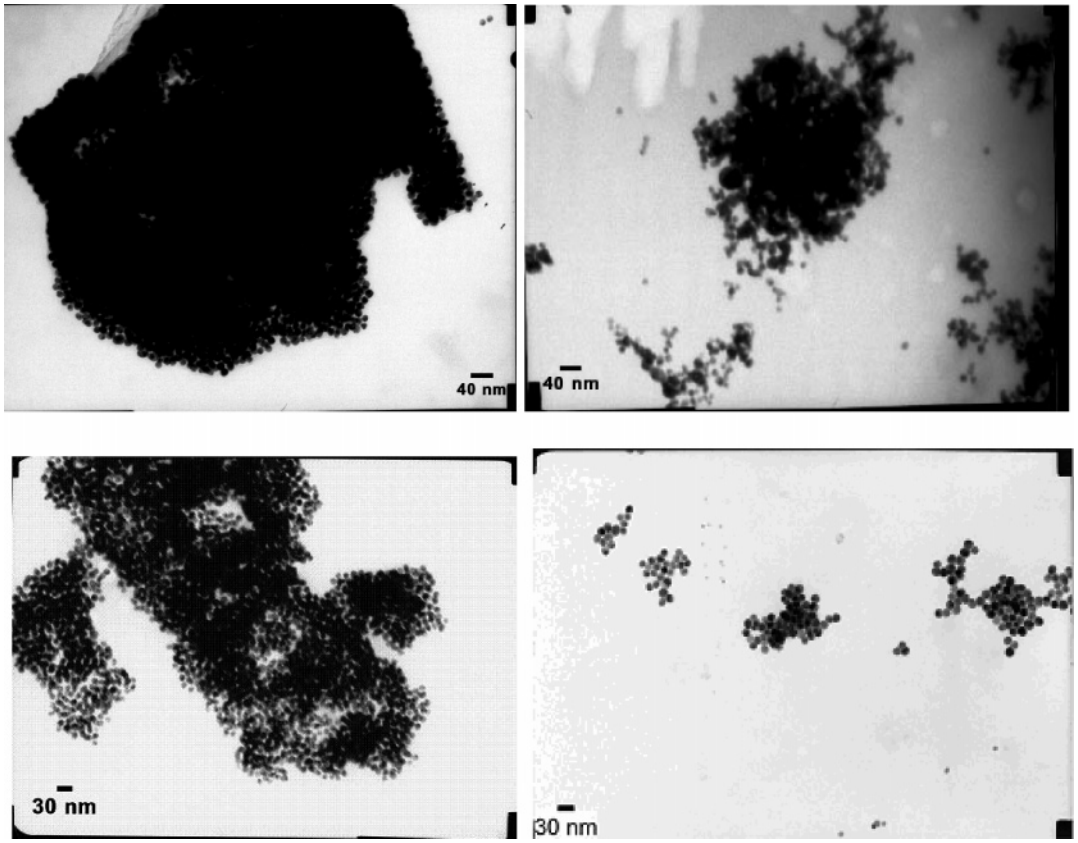

Figure 1. TEM images of gold nanoparticle aggregates prepared by addition of CTAB to an ~13-nm gold nanoparticle colloid, followed by stabilization with PVP. Nanoparticles within the aggregate can be seen to be approximately spherical in shape rather than ellipsoidal and in close physical proximity to each other.

Although there are numerous studies on the size dependence of electron relaxation in metal nanoparticles, the effect of aggregation or assembly of these nanoparticles on their electron−phonon relaxation dynamics has not been given much attention. Spatial and electromagnetic coupling between nanoparticles in an aggregate can be expected to have a considerable effect on the electron−phonon relaxation dynamics within these structures. For instance, Scherer and co-workers[33] studied the hot electron relaxation in thin films assembled from ~12-nm gold nanoparticles and demonstrated a decrease in the hot electron lifetimes with increasing aggregation, as characterized by the thickness of the nanoparticle film. Recently, Zhang and co-workers[34] observed coherent vibrational oscillation in gold nanoparticle aggregates prepared by the addition of Na_2S. The period of oscillation was found to increase as the probe wavelength was increased across the broadband absorption of the aggregates.

Although the optical properties of interacting nanoparticles have been studied mostly on nanoparticle assemblies formed on a substrate,[10,12,13,33,35] in this paper, we study the optical absorption and electron−phonon relaxation dynamics of stable aggregates of ~13-nm gold nanoparticles in solution. The solution has a wide distribution of aggregate sizes and fractal structures, as reflected in their broad absorption (550−700 nm) in addition to the characteristic plasmon absorption of the individual nanoparticles centered around 520 nm, in steady-state UV−visible extinction as well as in the transient absorption spectra. The electron−phonon relaxation dynamics within the aggregates, as measured by femtosecond transient absorption spectroscopy, is found to be significantly faster than that in the case of isolated gold nanoparticles and is seen to be probe wavelength-dependent. It has been suggested that probing at a particular wavelength interrogates a particular subset of the aggregates (with a particular size and/or fractal structure), that has a maximal absorption in the probe wavelength region.[34] Consistent with this suggestion, we find that as the probe wavelength is varied from 520 to 635 nm across the broadband absorption of the aggregates, the electron−phonon relaxation becomes progressively faster. Increase in the electron−phonon relaxation rate across the broad aggregate spectrum can be correlated to an enhanced overlap of the electronic oscillation frequency with the phonon spectrum as well as increased interfacial electron scattering with increasing extent of aggregation.

II. Experimental Section

Synthesis of Gold Nanoparticle Aggregates. Gold nanoparticles (13.1 ± 1.3 nm) were prepared by the citrate reduction of chloroauric acid.[36] Solution-stable nanoparticle aggregates were synthesized by the controlled addition of cationic surfactant cetyl trimethyl ammonium bromide (CTAB) (commonly used as a template in gold nanorod synthesis[37]) to the gold colloid in order to neutralize the negatively charged citrate-capped surface of the nanoparticles and thus initiate their aggregation (Figure 1).[38] To prevent the formation of very large aggregates, which eventually precipitate out, polyvinyl-pyrrolidone (PVP) was added to the solution as a stabilizing agent and the solution was allowed to aggregate for several days. Typically, 4 uL of a 0.5 mM solution of CTAB was added to 1 mL of the gold colloid with a nanoparticle concentration of ~11 nM, followed by addition of PVP (av MW = 55 000) to the solution, up to a final concentration of 0.01 M. The solution was stirred and further allowed to aggregate for 6 days. The synthesized sample was characterized by its UV−visible extinction (400−800 nm)

on a Shimadzu UV-3101-PC spectrophotometer in transmission mode. A dilute solution of the nanoparticle aggregates was spotted on a carbon-coated copper grid and imaged by TEM (Figure 1).

Pump−Probe Study of Hot Electron Relaxation Dynamics in Nanoparticle Aggregates. To study electron−phonon relaxation dynamics in gold nanoparticle aggregates by femtosecond transient absorption spectroscopy,[23] a pump−probe setup was employed. A frequency-doubled Nd:vanadate laser (Coherent Verdi) was used as the pump for the Ti:sapphire laser system (Clark MXR CPA 1000), which generated laser pulses of 100-fs duration (fwhm) with energy of 1 mJ at 800 nm at a repetition rate of 1 kHz. The pump beam was chopped mechanically with a light beam chopper (HMS 221). The second harmonic of the 800-nm fundamental at 400 nm was used as the pump for the optical excitation of the nanoparticle aggregates in solution placed under constant stirring in an optical cell (path length = 2 mm). The diameter of the laser focus spot on the sample was 100 μm. The laser pump pulse energy used in the experiments was reduced to less than 250 nJ with neutral density filters. A white-light continuum generated by focusing a small portion (4%) of the 800-nm fundamental beam of the Ti:sapphire laser into a 1-mm sapphire plate was used to probe the transient absorption of the sample at various delay times (t). The differential transmission signal, $S(t)$, was recorded with a pair of silicon photodiodes (Thorlab) and a lock-in amplifier (Stanford Research Systems). The recorded signal, $S(t)$, can be expressed as

$$S(\lambda, t) = \Delta T/T = (I_{\lambda,t} - \mathrm{I}_{\lambda,0})/\mathrm{I}_{\lambda,0}$$

where $\Delta T/T$ is the percent change in the transmission of probe light, $I_{\lambda,t}$ is the intensity of the probe light at wavelength λ after a delay time t from the pump laser heating pulse, and $I_{\lambda,0}$ is the intensity of the probe light at λ without the pump. As a result, the recorded signal, $S(\lambda, t)$, represents a transient bleach, which results from the optical excitation of the free electron distribution within the nanoparticles. Using this setup, the transient absorption spectra (300−800 nm) of the aggregate solution at delay times of 0, 1, and 2 ps were recorded. It is known that the fast decay component of the transient bleach is a direct measure of the electron−phonon relaxation within the nanoparticle. Following this procedure, electron−phonon relaxation dynamics in thiolated-DNA-modified gold nanoparticles was measured for different pump−pulse energies in the low fluence regime and compared to the dynamics in isolated gold nanoparticles. The isolated gold nanoparticles were probed at their plasmon maximum at 520 nm, whereas the nanoparticle aggregates were probed at four different wavelengths (530, 565, 600, and 635 nm) across their broadband absorption.

III. Results and Discussion

A. Plasmon Absorption in Gold Nanoparticle Aggregates. Figure 2 shows the UV−visible extinction spectra (400−800 nm) of a solution of isolated ∼13-nm gold nanoparticles (Figure 2a) and a solution of ∼13-nm gold nanoparticle aggregates (Figure 2b). As compared to the gold nanoparticle colloid, the aggregate solution shows a broadened absorption at longer wavelengths (550−700 nm) with respect to the single particle surface plasmon resonance maximum at 520 nm (Figure 3). The observation of a red-shifted spectral structure in aggregated nanoparticles is well-known in the literature as being due to interactions between the closely spaced nanoparticles[39,40] within the aggregates. The organic molecules CTAB and PVP do not have visible absorption to account for the spectral changes on aggregation. We observed similar spectral features when aggregation was carried out by addition of an electrolyte (e.g., NaCl) to the citrate-capped nanoparticles or on addition of excess single-stranded DNA oligonucleotides that bind to the gold nanoparticle surface and link them together.[41] Previous studies have also shown very similar spectral features in closely assembled gold nanoparticle structures.[12,13] The transient absorption spectrum (Figure 2c) of the nanoparticle aggregates shows a peak at 528 nm due to a transient bleach resulting from the femtosecond optical excitation of the metal free electrons, similar to that seen in isolated gold nanoparticles.[23] However, an additional shoulder in the 550−650 nm range can be seen clearly in the aggregate transient absorption.

The red-shifted absorption resulting from the aggregation, as confirmed by estimations of Mie extinction from nanoparticle clusters, is due to strong dipolar electromagnetic (EM) coupling between the plasmons of closely spaced nanoparticles in the aggregate (as seen in Figure 1), thus shifting the net plasmon resonance to lower frequencies.[42] The extent of the plasmon absorption shift depends on the degree of interparticle coupling within an individual aggregate; consequently, the plasmon resonance is at relatively longer wavelengths for larger aggregate sizes and aggregate structures with closely spaced nanoparticles.[43] The absorption of the aggregate solution is broad because of the contribution from various absorption subbands corresponding to different aggregate sizes and/or fractal structures, distributed in the solution. We expected relaxation dynamics of the nanoparticle aggregates to be different when probed at different wavelengths along the broad absorption band seen in their steady-state UV−vis and transient absorption spectra.

B. Electron−Phonon Relaxation Dynamics in Gold Nanoparticle Aggregates. Figure 3 shows the transient bleaching dynamics of the nanoparticle aggregates probed at 530 nm for two different pulse energies, that is, 40 nJ/pulse and 90 nJ/pulse. It is well known that the rise of the transient bleach is a result of electron−electron scattering within the gold nanoparticles on the time scale of 300−500 fs, whereas the fast decay of the transient bleach can be related directly to the dynamics of relaxation of the photoexcited electrons by exchanging energy with the nanoparticle phonon modes on the time-scale of ∼1 ps and slower decay because of phonon−phonon coupling on longer time scales ∼100 ps within the nanoparticles.[44,45] The limited time resolution of our laser pump pulse (100 fs) does not allow us to study the much faster electron−electron scattering processes. The essential result in our experiments is thus the creation of an excited or hot electron distribution just after the pump pulse, which consequently relaxes by electron−phonon scattering. The rise and decay of the transient bleach kinetics are fit to an exponential function of the form

$$(1 - \exp(-t/\tau_r)) \exp(-t/\tau_d)$$

to obtain the rise time, τ_r (ps), and the decay time (or the hot electron lifetimes), τ_d (ps). The decay time at the higher power 90 nJ/pulse ($\tau_d = 1.72 \pm 0.09$ ps) is longer than that at 40 nJ/pulse ($\tau_d = 1.64 \pm 0.07$ ps). Thus, the pump−probe dynamics of the aggregates shows a power dependence similar to that seen in isolated gold nanoparticles as attributed to the linear dependence of the electronic heat capacity on the hot electron temperature.[25,27,44,45] The laser energy dependence of the electron−phonon relaxation time in the 13-nm isolated gold nanoparticles is shown separately in Figure 4. The extrapolated zero power limit of the electron−phonon relaxation time in the

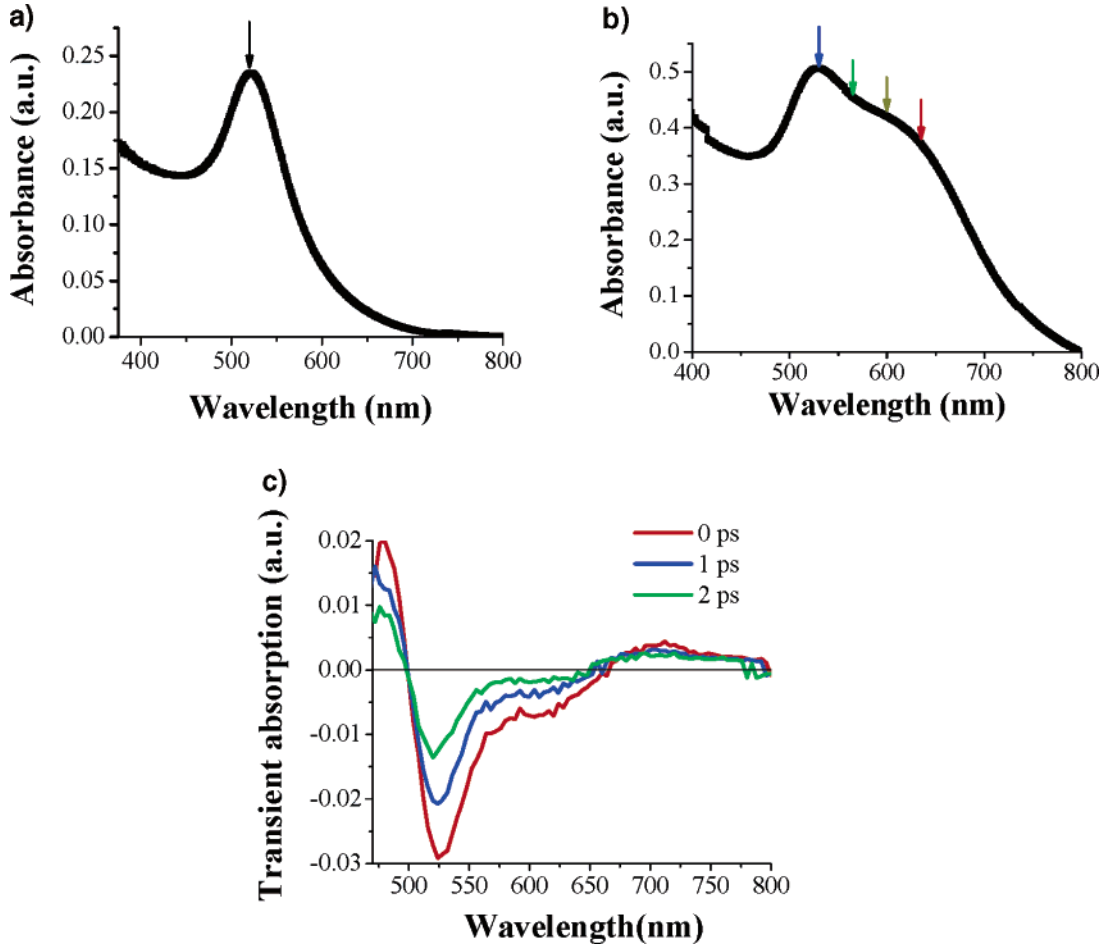

Figure 2. (a) UV−visible extinction spectrum of (a) an ∼13-nm gold nanoparticle colloid, showing a peak absorption at 520 nm due to the surface plasmon resonance for isolated 13-nm nanoparticles (b) UV−visible extinction spectrum of a solution of ∼13-nm gold nanoparticle aggregates showing a broad absorption in the 550−700-nm region, in addition to the plasmon band at 520 nm. The arrows indicate different wavelengths across the broadband absorption, at which the aggregates were probed for the femtosecond transient bleach dynamic studies in Figure 4. (c) Transient absorption bleach spectra of gold nanoparticle aggregates recorded at delay times of 0, 1, and 2 ps after optical excitation by a 400-nm 100-fs pulse. In addition to the peak in the transient bleach at 528 nm, a broad shoulder in the range 550−650 nm can be distinctly seen.

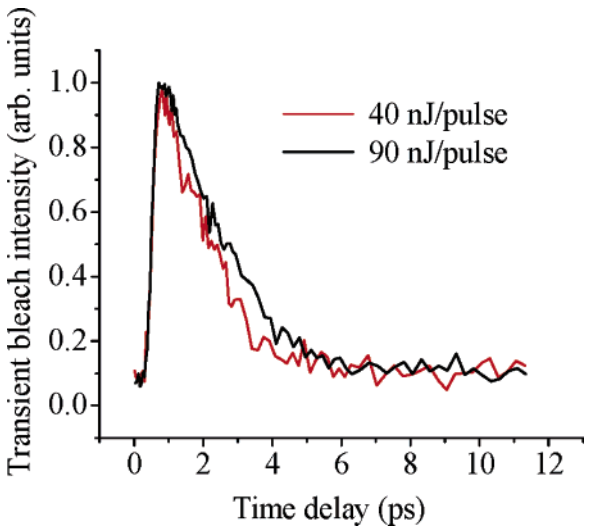

Figure 3. Power-dependence of transient bleach dynamics in gold nanoparticle aggregates probed at 530 nm. 100-fs pulses at 400 nm were used as the pump at two different pulse energies, 40 nJ/pulse (red) and 90 nJ/pulse (black). The rise and decay of the transient bleaching were fit to an exponential function of the form $(1 - \exp(-t/\tau_r))\exp(-t/\tau_d)$ to obtain a hot electron lifetime, τ_d, of 1.64 ± 0.07 ps at 37 nJ/pulse and 1.72 ± 0.09 ps at 90 nJ/pulse.

13-nm nanoparticles is determined to be 0.68 ps, which is consistent with earlier results from our lab[44] and others.[46]

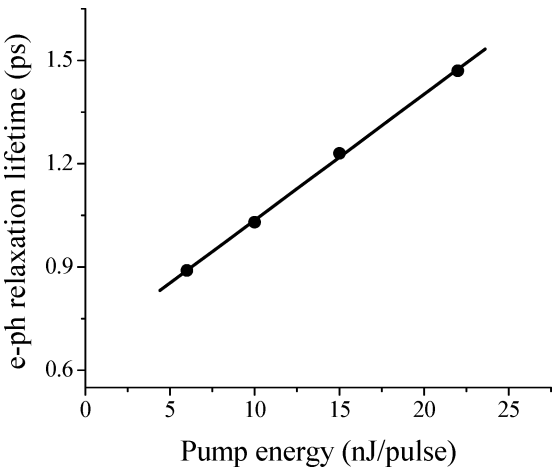

Figure 4. Laser pump energy (nJ/pulse) dependence of the electron−phonon relaxation time (ps) in 13-nm gold nanoparticles in the low fluence regime. 100-fs pulses at 400 nm were used as the pump while the probe wavelength was 521 nm corresponding to the plasmon absorption maximum of the nanoparticles. The black line in the plot is a straight line fit to the data with an intercept of 0.68 ps, corresponding to the zero power limit of the electron−phonon relaxation time in the 13-nm gold nanoparticles.

The electron−phonon relaxation dynamics within the aggregates at different probe wavelengths (530, 565, 600, and 635 nm) and that in isolated gold nanoparticles (probed at 520 nm)

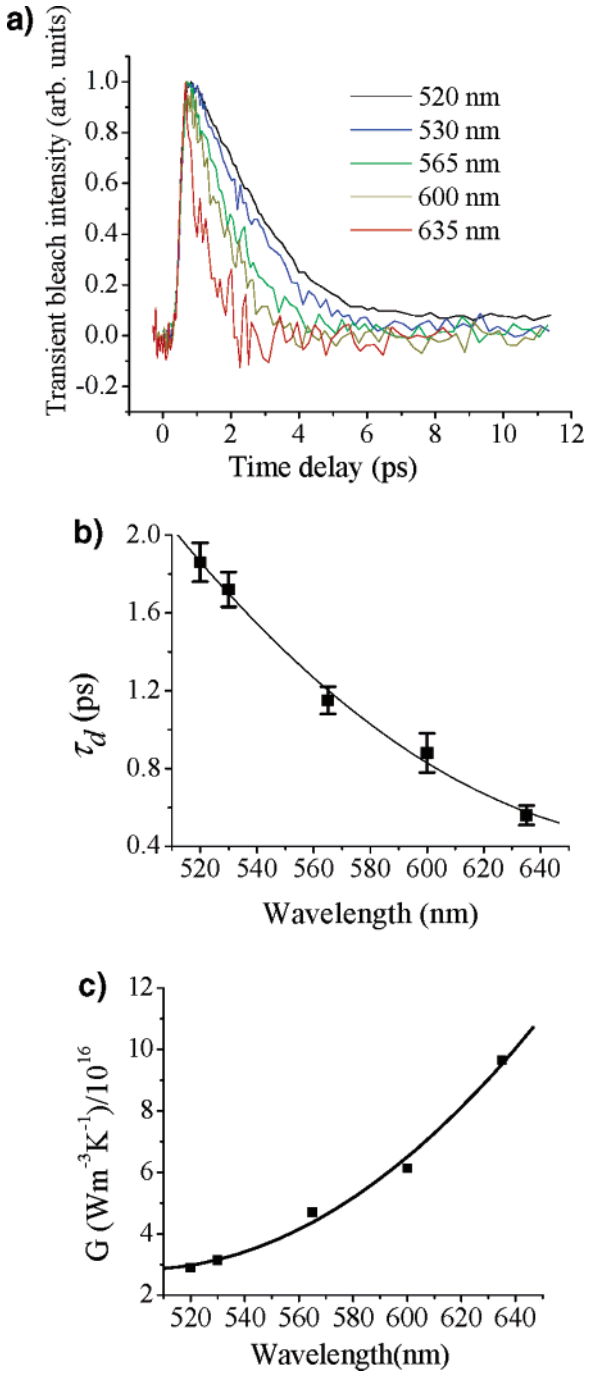

Figure 5. (a) Transient bleach dynamics in isolated gold nanoparticles at 520 nm (black) and that in gold nanoparticle aggregates probed at 530 (blue), 665 (green), 600 (yellow), and 635 nm (red). 100-fs pulses at 400 nm with an energy of 90 nJ/pulse were used as the pump. The rise and decay of the transient bleaching were fit to an exponential function of the form $(1 - \exp(-t/\tau_r))\exp(-t/\tau_d)$ to obtain the hot electron lifetime, τ_d (ps), for each case. Note that the optical densities of the aggregate solution and the gold nanoparticle colloid at the pump wavelength, 400 nm, were adjusted to be similar to ensure that both samples reach a similar hot electron temperature by optical pumping at 90 nJ/pulse, allowing direct comparison of the electron relaxation dynamics (b) Plot of measured hot electron lifetimes τ_d (ps) and (c) calculated electron−phonon coupling constants, G (Wm^{-3}K^{-1})/10^{16}, against varying degree of aggregation, as characterized by the probe wavelength (nm). The vertical error bars in b indicate the standard deviation of the exponential fit of the decay curves in a. The black curves in b and c are guides for the eye.

has been compared at a pulse energy of 90 nJ/pulse in Figure 5a. The figure shows a faster electron−phonon relaxation in the nanoparticle aggregates as compared to that in isolated gold nanoparticles ($\tau_d = 1.86 + 0.10$ ps) at the same pulse energy. This is also observed for nanoparticle aggregates prepared by other methods. In addition, the electron−phonon relaxation rate in the aggregates becomes faster at progressively longer probe wavelengths. It has been widely suggested in the literature that by probing at a particular wavelength along the broad absorption band of aggregates, one can interrogate a particular size/local fractal structure of the aggregates within the inhomogeneous absorption band.[34] This suggestion has been verified by burning of spectral holes in the broad aggregate absorption by irradiating the aggregates at a particular wavelength.[34,47] Accordingly, our experimental results demonstrate that the electron relaxation dynamics can be probed independently within a subset of aggregate sizes/structures by using a probe wavelength close to the absorption of that subset. The trend of the hot electron lifetimes with the probe wavelength, shown in Figure 5b, thus indicates that electron−phonon relaxation is relatively faster within those aggregates with greater interparticle coupling (due to either a larger aggregate size or closely spaced nanoparticles) and, hence, absorbing at longer wavelengths. This is in good agreement with the observations of Scherer and co-workers on the electron dynamics in thin films assembled from ~12-nm gold nanoparticles; electron relaxation dynamics was observed to get faster with increasing extent of nanoparticle aggregation within the films.[33] Although Scherer and co-workers characterized the extent of aggregation/internanoparticle coupling by the thickness of the aggregated film, we have employed different probe wavelengths to selectively interrogate structures with varying extent of aggregation, distributed within the same solution. Similarly, Zhang and co-workers observed a variation of the coherent phonon oscillation period within gold nanoparticle aggregate structures because they probed at different wavelengths across the broad aggregate absorption; however, they did not find any variation in the electron−phonon relaxation dynamics itself.[34]

The value of the electron−phonon coupling constant, G (W/m^{-3}K^{-1}), for the nanoparticle aggregates can be calculated from their hot electron lifetimes, τ_d, as per the two-temperature model (TTM),[20] which considers the hot electron gas and the lattice to be two coupled subsystems and is generally valid for time scales longer than the electron−electron scattering processes. In the low fluence approximation, the TTM model gives

$$G = C_e/\tau_d$$

where C_e is the electronic heat capacity (Jm^{-3}K^{-1}). On the basis of a value of C_e for gold of 2.0×10^4 Jm^{-3}K^{-1} at room temperature and the extrapolated zero power decay time of 0.68 ps from Figure 4, the electron−phonon coupling constant, G, for 13-nm gold nanoparticles is estimated to be 2.90×10^{16} Wm^{-3}K^{-1}. The value of C_e at the 90 nJ/pulse is calculated to be 5.4×10^4 Jm^{-3}K^{-1} from the measured hot electron lifetime $\tau_d = 1.86$ ps for isolated 13-nm gold nanoparticles at the 90 nJ/pulse. Using this value of C_e at the 90 nJ/pulse, the electron−phonon coupling constants can be estimated for the aggregates for the different probe wavelength cases. Figure 5c shows the trend of the calculated electron−phonon coupling constant, G, for the aggregates increasing with the interrogating probe wavelength. It can be seen that the value of G for the aggregates supersedes the bulk value of $\sim 3.0 \times 10^{16}$ W/m^{-3}K^{-1}.

C. Dependence of Hot Electron Lifetime on the Degree of Aggregation. To explain the dependence of the hot electron lifetimes on the extent of nanoparticle aggregation, the mechanism of electron−phonon relaxation within the nanoparticles

of the aggregate must be analyzed. Electron−phonon relaxation within nanoparticles has two pathways: first, scattering of the excited electron by the nanoparticle lattice phonons and, second, inelastic scattering of hot electrons at the surface of the nanoparticles. Both of these pathways contribute to the net observed electron−phonon coupling constant, G.[48] The effectiveness of electron−phonon scattering has been suggested to depend inversely on the electron oscillation frequency-phonon resonance detuning (*EOPRD*) within a nanostructural domain.[49] The effective oscillation frequency arises from elastic scattering of electrons from the domain boundary. The spectral overlap of the electron oscillation frequency with the phonon spectrum governs the efficient exchange of energy between the electron and phonon baths. EOPRD can be expressed as

$$EOPRD = \upsilon_f / d - \omega_d$$

where υ_f is the Fermi velocity of the electrons in gold, ω_d is the Debye frequency for gold, and d is the size of the domain or the distance over which the hot electrons are delocalized within the nanostructure. With increasing degree of aggregation, the aggregate size, d, increases, resulting in a decrease in the electron oscillation frequency and a lower *EOPRD* (thus, better electron−phonon spectral overlap). The e-ph coupling constants thus increase with greater extent of aggregation, starting from the value for an isolated nanoparticle toward the bulk value for gold. At the same time, hot electrons delocalized over a nanoparticle aggregate can be expected to undergo much more enhanced inelastic scattering at the interface of the particles, as compared to the case of isolated nanoparticles.[33] With a greater degree of nanoparticle aggregation, a greater extent of interfacial scattering can be expected, leading to a further increase in the electron relaxation rates, even beyond the bulk value. Such an explanation is analogous to the finding of El-Sayed Ali et al.[50] of higher electron relaxation rates in polycrystalline gold films as compared to single gold crystals, attributed to additional electron scattering at grain boundaries. Our experimental results thus suggest that the electrons in the nanoparticle aggregate are not restricted to a single colloidal particle; they are mobile over the aggregated domains, as originally suggested by Scherer and co-workers.[33] Apart from the well-known dipolar plasmon coupling, significant electronic coupling can thus be seen between closely interacting nanoparticles.

IV. Conclusions

We studied the ultrafast dynamics in solution-stable aggregates of ∼13-nm gold nanoparticles by femtosecond laser pump−probe spectroscopy. UV−visible extinction and transient absorption of the nanoparticle aggregates showed an extended plasmon broadband absorption in the 550−700-nm region, in addition to the isolated gold nanoparticle plasmon resonance because of absorption contributions from aggregates with different sizes and/or different fractal structures. The aggregates showed a electron−phonon relaxation rate that was faster than that in isolated gold nanoparticles and also probe-wavelength dependent. As the probe wavelength was varied from 520 to 635 nm across the broad aggregate absorption, the electron−phonon relaxation became faster. Thus, each wavelength can selectively interrogate a subset of aggregate sizes/structures with an absorption around that wavelength. Our results thus support the proposition that optical excitations within the broad distribution of nanoparticle aggregates are localized in small subwavelength regions (also known as hot spots), a phenomenon that can be potentially useful in optical writing of data within these nanostructures.[47] We also correlated the increase in electron−phonon relaxation rate with increasing probe wavelength to an increase in electron oscillation-phonon spectral overlap and interfacial scattering with increasing extent of aggregation. Our results may be potentially useful for tuning hot electron lifetimes to fast response in nanoparticle assemblies and for optoelectronic device and photochemical applications.

Acknowledgment. We thank Xiaohua Huang and Qusai Darugar for obtaining TEM images of the gold nanoparticle aggregates. This work is supported by the Materials Research Division of the National Science Foundation (no. 0138391).

References and Notes

(1) Kelly, K. L.; Coronado, E.; Zhao, L. L.; Schatz, G. C. *J. Phys. Chem. B* **2003**, *107*, 668.
(2) Kreibig, U.; Vollmer, M. *Optical Properties of Metal Clusters*, Springer, New York, 1995.
(3) Wei, Q.-H.; Su, K.-H.; Durant, S.; Zhang, X. *Nano Lett.* **2004**, *4*, 6.
(4) Mirkin, C. A. *Inorg. Chem.* **2000**, *39*, 2258.
(5) Sastry, M.; Rao, M.; Ganesh, K. N. *Acc. Chem. Res.* **2000**, *35*, 847.
(6) Alivisatos, A. P.; Johnsson, K. P.; Peng, X.; Wilson, T. E.; Loweth, C. J.; Bruchez, M. P., Jr.; Schultz, P. G. *Nature* **1996**, *382*, 609.
(7) Mirkin, C. A.; Letsinger, R. L.; Mucic, R. C.; Storhoff, J. J. *Nature* **1996**, *382*, 607.
(8) Collier, C. P.; Saykally, R. J.; Shiang, J. J.; Henrichs, S. E.; Heath, J. R. *Science* **1997**, *277*, 1978.
(9) Grabar, K. C.; Freeman, R. G.; Hommer, M. B.; Natan, M. J. *Anal. Chem.* **1995**, *67*, 735.
(10) Félidj, N.; Aubard, J.; Lévi, G.; Krenn, J. R.; Hohenau, A.; Schider, G.; Leitner, A.; Aussenegg, F. R. *App. Phys. Lett.* **2003**, *82*, 3095.
(11) Dimon, P.; Sinha, S. K.; Weitz, D. A.; Safinya, C. R.; Smith, G. S.; Varady, W. A.; Lindsay, H. M. *Phys. Rev. Lett.* **1986**, *57*, 595.
(12) Westcott, S. L.; Oldenburg, S. J.; Lee, T. R.; Halas, N. J. *Chem. Phys. Lett.* **1999**, *300*, 651.
(13) Félidj, N.; Truong, S. L.; Aubard, J.; Lévi, G.; Krenn, J. R.; Hohenau, A.; Leitner, A.; Aussenegg, F. R. *J. Chem. Phys.* **2004**, *120*, 7141.
(14) Poliakov, E.; Shalaev, V. M.; Shubin, V.; Markel, V. A. *Phys. Rev. B* **1999**, *60*, 10739.
(15) Haus, J.; Kalyaniwalla, N.; Inguva, R.; Bloemer, M.; Bowden, C. M. *J. Opt. Soc. Am. B* **1989**, *6*, 787.
(16) Hagfeldt, A.; Grätzel, M. *Chem. Rev.* **1995**, *95*, 49.
(17) Cavanagh, R. R.; King, D. S.; Stephenson, J. C.; Heinz, T. F. *J. Phys. Chem.* **1993**, *97*, 786.
(18) Heilweil, E. J.; Hochstrasser, R. M. *J. Chem. Phys.* **1985**, *82*, 4762.
(19) Schoenlin, R. W.; Lin, W. Z.; Fujimoto, J. G.; Eesley, G. J. *Phys. Rev. Lett.* **1987**, *58*, 1680.
(20) Sun, C.-K.; Vallee, F.; Acioli, L. H.; Ippen, E. P.; Fujimoto, J. G. *Phys. Rev. B* **1993**, *48*, 12365.
(21) Kaveh, M.; Wiser, N. *Adv. Phys.* **1984**, *33*, 257.
(22) Hodak, J. H.; Henglein, A.; Hartland, G. V. *J. Phys. Chem. B* **2000**, *104*, 9954.
(23) Ahmadi, T. S.; Logunov, S. L.; El-Sayed, M. A. *J. Phys. Chem.* **1996**, *100*, 8053.
(24) Roberti, T. W.; Smith, B. A.; Zhang, J. Z. *J. Chem. Phys.* **1995**, *102*, 3860.
(25) Logunov, S. L.; Ahmadi, T. S.; El-Sayed, M. A.; Khoury, J. T.; Whetten, R. L. *J. Phys. Chem. B* **1997**, *101*, 3713.
(26) Link, S.; Burda, C.; Mohamed, M. B.; Nikoobakht, B.; El-Sayed, M. A. *Phys. Rev. B* **2000**, *61*, 6086.
(27) Hodak, J. H.; Martini, I.; Hartland, G. V. *Chem. Phys. Lett.* **1998**, *284*, 135.
(28) Hodak, J. H.; Henglein, A.; Hartland, G. V. *J. Chem. Phys.* **1999**, *111*, 8613.
(29) Del Fatti, N.; Flytzanis, C.; Vallee, F. *Appl. Phys.* B **1999**, *68*, 433.
(30) Stella, A.; Nisoli, M.; de Silvestri, S.; Svelto, O.; Lanzani, G.; Cheyssac, P.; Kofman, R. *Phys. Rev. B* **1996**, *53*, 15497.
(31) Nisoli, M.; Stagira, S.; de Silvestri, S.; Stella, A.; Togini, P.; Cheyssac, P.; Kofman, R. *Phys. Rev. Lett.* **1997**, *53*, 3575.
(32) Perner, M.; Bost, P.; Plessen, G. V.; Feldmann, J.; Becker, U.; Mennig, M.; Schmidt, H. *Phys. Rev. Lett.* **1997**, *78*, 2192.
(33) Feldstein, M. J.; Keating, C. D.; Liau, Y.-H.; Natan, M. J.; Scherer, N. F. *J. Am. Chem. Soc.* **1997**, *119*, 6638.
(34) Grant, C. D.; Schwartzberg, A. M.; Norman, T. J., Jr.; Zhang J. Z. *J. Am. Chem. Soc.* **2003**, *125*, 549.
(35) Eah, S.-K.; Jaeger, H. M.; Scherer, N. F.; Lin, X.-M.; Wiederrecht, G. P. *Chem. Phys. Lett.* **2004**, *386*, 390.

(36) Turkevich, J.; Stevenson, P. C.; Hillier, J. *Discuss. Faraday Soc*. **1951**, *11*, 55.
(37) Jana, N. R.; Gearheart, L.; Murphy, C. *J. Phys. Chem. B* **2001**, *105*, 4065.
(38) Pal, A.; Ghosh, S. K.; Esumi, K.; Pal, T. *Langmuir* **2004**, *20*, 575.
(39) Rechberger, W.; Hohenau, A.; Leitner, A.; Krenn, J. R.; Lamprecht, B.; Aussenegg, F. R. *Opt. Commun.* **2003**, *220*, 137.
(40) Su, K.-H.; Wei, Q.-H. Zhang, X.; Mock, J. J.; Smith, D. R.; Schultz, S. *Nano Lett.* **2003**, *3*, 1087.
(41) Storhoff, J. J.; Elghanian, R.; Mirkin, C. A.; Letsinger, R. L. *Langmuir* **2002**, *18*, 6666.
(42) Quinten, M.; Kreibig, U. *Surf. Sci*. **1986**, *172*, 557.
(43) Lazarides, A. A.; Schatz, G. C. *J. Phys. Chem. B* **2000**, *104*, 460.
(44) Link, S.; El-Sayed, M. A. *J. Phys. Chem. B* **1999**, *103*, 8410.
(45) Link, S.; El-Sayed, M. A. *Annu. Rev. Phys. Chem*. **2003**, *54*, 331.
(46) Qui, T. Q.; Tien, C. L. *Int. J. Heat Mass Transfer* **1992**, *35*, 719.
(47) Safonov, V. P.; Shalaev, V. M.; Markel, V. A.; Danilova, Y. E.; Lepeshkin, N. N.; Kim, W.; Rautian, S. G.; Armstrong, R. L. *Phys. Rev. Lett*. **1998**, *80*, 1102.
(48) Smith, B. A.; Zhang, J. Z.; Giebel, U.; Schmid, G. *Chem. Phys. Lett*. **1997**, *270*, 139.
(49) Gorban, S. A.; Nepijko, S. A.; Tomchuk, P. M. *Int. J. Electron*. **1991**, *70*, 485.
(50) Juhasz, T.; Elsayed-Ali, H. E.; Smith, G. O.; Suárez, C.; Bron, W. E. *Phys. Rev. B* **1993**, *48*, 15488.